Journal of Power Sources 217 (2012) 170–174

Contents lists available at SciVerse ScienceDirect

Journal of Power Sources

journal homepage: www.elsevier.com/locate/jpowsour

Electrochemical behavior of mixed conducting oxide cathode on oxygen excess-type solid electrolyte

Takayoshi Mitsui [a], Atsushi Mineshige [a,*], Takahiro Funahashi [a], Hiroyuki Mieda [a], Yusuke Daiko [a], Masafumi Kobune [a], Hideki Yoshioka [b], Tetsuo Yazawa [a]

[a] Department of Materials Science and Chemistry, Graduate School of Engineering, University of Hyogo, 2167 Shosha, Himeji, Hyogo 671-2201, Japan
[b] Hyogo Prefectural Institute of Technology, Suma-ku, Kobe, Hyogo 654-0037, Japan

HIGHLIGHTS

► $(La_{0.6}Sr_{0.4})(Co_{0.8}Fe_{0.2})O_3$ was good cathode for lanthanum silicate electrolytes.
► By Introducing Ag nanoparticles to LSCF, electrode property was largely improved.
► Ag-modified LSCF showed quite small activation energy for polarization resistance.

ARTICLE INFO

Article history:
Received 2 April 2012
Received in revised form
21 May 2012
Accepted 28 May 2012
Available online 1 June 2012

Keywords:
Solid oxide fuel cell
Lanthanum silicate
Apatite-type electrolyte
Oxygen reduction
Silver nano-particles

ABSTRACT

Electrochemical oxygen reduction behavior for a half cell composed of a mixed ionic and electronic conducting (MIEC) oxide and an oxygen excess-type solid electrolyte was investigated. A perovskite-type MIEC oxide, $(La_{0.6}Sr_{0.4})(Co_{1-y}Fe_y)O_{3-\delta}$ (LSCF), was employed as a base material for an electrode catalyst of oxygen reduction reaction. As an electrolyte, Al-doped lanthanum silicate $[La_{10}(Si_{5.8}Al_{0.2})O_{26.9}$ (ALSO)] was used, which is a new class of oxide ion conductors with apatite-type structure. The evaluated polarization resistance, R_{pol}, for the reaction largely depended on y, and the minimum resistance was obtained for $y = 0.2$. The R_{pol} value was 0.3 Ω cm^2 at 1073 K in ambient air [$P(O_2) = 2.1 \times 10^4$ Pa] for $y = 0.2$. To improve the performance, introduction of silver nano-particles onto the LSCF particles was studied. With the Ag-modification, R_{pol} at 1073 K could be minimized toward 0.08 Ω cm^2. The cathodic overpotential of the electrode evaluated from DC polarization at 1073 K was 18 mV at 0.1 A cm^{-2}.
© 2012 Elsevier B.V. All rights reserved.

1. Introduction

Nakayama et al. [1–3] discovered a new class of oxide ion conductors with apatite-type structure, lanthanoid silicates, $Ln_{9.333+x}Si_6O_{26+1.5x}$, in 1995. The apatite-type solid electrolytes have recently attracted considerable interest because of their high ionic conductivity. In addition, their conducting mechanism is of interest since it is quite different from the simple oxygen vacancy diffusion of typical oxide ion conductors. The most striking point is that ion conduction is achieved via oxygen interstitials. The second is concerned with anisotropic conductivity: [4] *i.e.*, conductivity could be enhanced by preferential orientation of the crystal along the conducting channel. A unit cell of the representative oxide, lanthanum silicate ($La_{9.333+x}Si_6O_{26+1.5x}$, LSO) based on hexagonal oxyapatite-type $A_5(BO_4)_3O$ structure ($P6_3/m$) is shown in Fig. 1 using VESTA software [5]. It consists of 10 lanthanum atoms including 2/3 vacancies, 6 SiO_4 tetrahedra, and another 2 oxygen atoms along the c-axis. By introducing extra lanthanum atoms into the lanthanum vacancies, oxygen interstitials (not shown) appear as excess oxide ions, which are believed to contribute to the ionic conduction, especially along its c-axis.

Slight cation doping into the Si-site was found to be effective for the improvement in oxide ion conductivity [6–8]. We have shown that the oxygen excess-type Al-doped LSO, $La_{10}(Si_{5.8}Al_{0.2})O_{26.9}$ on weighted basis (OE-ALSO) was the best composition as a solid electrolyte [9] because of its high electrical conductivity (6.3×10^{-2} S cm^{-1} at 1073 K [10]), high ionic transport number (>0.996 at 1073 K [10,11]), high chemical stability under presence of carbon dioxide as well as under the reducing conditions [12], and high ability to construct efficient electrode/electrolyte interfaces using MIEC electrode [10]. In addition, we have examined its

* Corresponding author. Tel./fax: +81 79 267 4944.
E-mail address: mine@eng.u-hyogo.ac.jp (A. Mineshige).

0378-7753/$ – see front matter © 2012 Elsevier B.V. All rights reserved.
http://dx.doi.org/10.1016/j.jpowsour.2012.05.094

potential as the solid oxide fuel cell (SOFC) electrolyte, and reported that a maximum power density of ca. 0.25 W cm^{-2} could be drawn from an SOFC unit cell based on OE-ALSO (0.72 mm thick) operating at 1073 K [10]. From the view point of the element strategy and green and sustainable development, LSO is also attractive because one of major constituent atoms of this electrolyte is environment friendly and common element, silicon. Therefore, this kind of materials is one of the good candidate for high temperature electrochemical devices such as SOFCs and sensors. However, electrochemical behavior of this material with electrode catalysts has not yet been well understood. To investigate this is quite important for the understanding of an electrode/electrolyte system with an oxygen-excess type material as well as for the construction of a high performance SOFC. In the present study, cathode materials for this electrolyte were examined. A well-known MIEC conductor, $(La_{0.6}Sr_{0.4})(Co_{1-y}Fe_y)O_{3-\delta}$ (LSCF, $0.0 \le y \le 1.0$), was used as the base material for cathode.

2. Experimental

The OE-ALSO solid electrolyte, $La_{10}(Si_{5.8}Al_{0.2})O_{26.9}$, was synthesized via conventional solid-state reaction. Specimens were obtained from a mixture of raw powders of La_2O_3 (99.99% purity, Kishida Chemical Co., Ltd.), SiO_2 (99% purity, Kishida Chemical Co., Ltd.), and $Al(OH)_3$ (99.5% purity, Kishida Chemical Co., Ltd.). Finally, powders were pressed into a disk at 57 MPa, followed by sintering at 1973 K for 10 h in air as described elsewhere [10]. After the thickness of the obtained disk (17 mm in diameter) was adjusted to 1.0 mm, LSCF and platinum pastes were applied on each surface of the disk (electrode surface area: 0.38 cm^2), and used as working and counter electrodes, respectively. Platinum mesh plates were applied on both electrodes as current collectors. A platinum wire with 0.3 mm in diameter surrounding the circumference of the electrolyte pellet was used as a reference electrode. The electrode polarization resistance was evaluated with the AC impedance method using an electrochemical analyzer (ALS, 760C). The measuring temperature was 873–1073 K, and the surrounding atmosphere was air [$P(O_2) = 2.1 \times 10^4$ Pa]. The DC polarization measurement was also done using the same system, and fuel cell performance was evaluated with a galvanostat (Hokuto Denko, HA-151) and an electrometer (Advantest, R6452E).

To reduce electrode resistance, silver nano-particles were deposited on cathode materials. Sakito et al. [13] studied oxygen reduction reaction of LSCF on the $Ce_{0.9}Gd_{0.1}O_{1.9-\delta}$ electrolyte. They reported that large improvement in the performance of LSCF was seen when the modification by silver fine particles (<2 μm) into LSCF particles was done with an infiltration technique. Here, we investigated oxygen reduction behavior of the Ag-modified LSCF electrode applied on the LSO-based oxygen excess-type electrolyte by using the infiltration technique. For Ag-modification, a defined amount (M mg) of silver nitrate aqueous solution (0.64 mol dm^{-3}) was just dropped onto the cathode layer (0.38 cm^2) of a cell, and a cell was heat treated at 1073 K.

3. Results and discussion

3.1. Effect of Co/Fe ratio on electrochemical behavior

Fig. 2a shows AC impedance results for LSCF electrode/OE-ALSO electrolyte half cell at 1073 K using a 3-electrode configuration. Note that the ohmic resistance, R_{ohm}, has been subtracted from the measured response to compare the net electrode resistance. The remaining impedance could be roughly represented as a single semi-arc. In the present study, the electrode polarization resistance, R_{pol}, was assumed to be equal to the diameter of the semi-arc. The

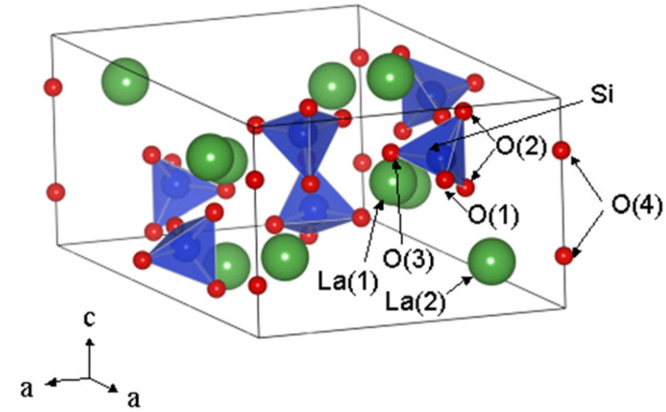

Fig. 1. Hexagonal apatite-type structure of $La_{9.333+x}Si_6O_{26+1.5x}$ drawn with VESTA software [5]. It consists of 10 lanthanum atoms including 2/3 vacancies, 6 SiO_4 tetrahedra and another 2 oxygen atoms along the c axis. By introducing extra lanthanum atoms into the lanthanum vacancies, oxygen interstitials (not shown) will appear as excess oxygen.

R_{pol} values were listed in Table 1 together with R_{ohm}. In the case of $y = 1.0$, the R_{pol} was 11.4 Ω (4.33 Ω cm^2). The R_{pol} was reduced with a decrease in y, and it was minimized to 0.8 Ω (0.3 Ω cm^2) at $y = 0.2$, This is because the catalytic activity of the cobalt redox couple (mainly Co^{3+} and Co^{4+}) was superior to that of iron. However, this value increased again in the region of $y < 0.2$, and it was 4.8 Ω (1.8 Ω cm^2) at $y = 0.0$. It is probably because chemical reaction or cation diffusion proceeded at the electrode/electrolyte interface in the case of the cobalt-rich composition. In addition, a degree of mismatch in thermal expansion coefficients (TECs) between electrode and electrolyte materials is important. The TEC for the LSO-

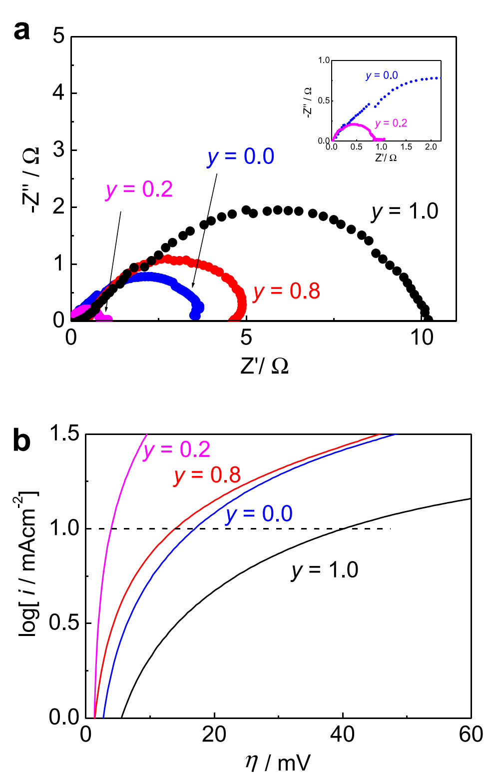

Fig. 2. (a) AC impedance plot (R_{ohm}-free) and (b) DC polarization curve (IR-free) for $(La_{0.6}Sr_{0.4})(Co_{1-y}Fe_y)O_{3-\delta}$ (LSCF, $0.0 \le y \le 1.0$) electrode/$La_{10}(Si_{5.8}Al_{0.2})O_{26.9}$ (OE-ALSO) electrolyte half cell at 1073 K using a 3-electrode configuration.

Table 1
Evaluated ohmic resistance, R_{ohm}, polarization resistance, R_{pol}, and overpotential, η from AC impedance and DC polarization methods as a function of Fe content (y) in LSCF for the LSCF/OE-ALSO half cell at 1073 K.

y	R_{ohm}/Ω	R_{pol}/Ω (Ω cm^2)	η/mV at 10 mA cm^{-2}
0.0	4.8	4.8 (1.8)	17.3
0.2	3.4	0.8 (0.3)	3.9
0.8	6.5	3.5 (1.3)	14.5
1.0	13.1	11.4 (4.33)	40.1

based materials have been investigated by Kharton et al. [14], and it was reported as ca 9-10 $\times$ 10^{-6} K^{-1}, which is similar to that for yttria-stabilized zirconia. The value for LSCF system increased with decreasing Fe content, y, and ranged between 12.6 $\times$ 10^{-6} ($y = 1.0$) to 19.7 $\times$ 10^{-6} ($y = 0.0$) [15]. Although the electrode property of $y = 0.2$ is good, there is a possibility that the performance degrade after heat cycles due to such a large mismatch at the interface. In addition, it is preferable to substitute cobalt by iron because of the cost and environmental reasons. In the next section, a method for the improvement of the performance of LSCF with $y = 0.8$ will be discussed.

Fig. 2b shows a current density-cathodic overpotential (η) plot for the same system at 1073 K under air evaluated with a DC polarization method. It should be noted that the *IR*-loss has been subtracted from the measured overvoltage. A similar tendency was obtained regarding Co/Fe ratio dependence on the electrode property between AC impedance and DC polarization methods. The η evaluated at 1073 K in air are added to Table 1. The value could be minimized when y was equal to 0.2. The η values under a current of 0.1 A cm^{-2} at 1073 K were 141 and 26 mV for $y = 0.8$ and 0.2, respectively. Since R_{ohm} also decreased with decreasing y according to the AC impedance measurements (see Table 1), the one of the main factor to increase R_{pol} was thought to be ununiform current distribution at the Pt mesh current collector/electrode interface due to a lack of electronic conductivity of LSCF. We have previously investigated the electronic conductivity for the LSCF system in detail. Those for LSCF ($y = 0.0$ and 0.8) were 1.2 $\times$ 10^3 [16] and 2.6 $\times$ 10^2 S cm^{-1} [17] at 1073 K in air, respectively. Hence, enhancement in the electronic conductivity as well as the catalytic activity of LSCF is proved to be important to improve the electrochemical behavior. Fig. 3 shows cross-sectional SEM image of the LSCF ($y = 0.8$)/OE-ALSO interface. The thickness of LSCF layer was about 40 μm, containing uniform pores throughout the material. Since structural deformations or cracks at the interface or in the layer were not observed, it was found that an ideal interface could be fabricated in the present study.

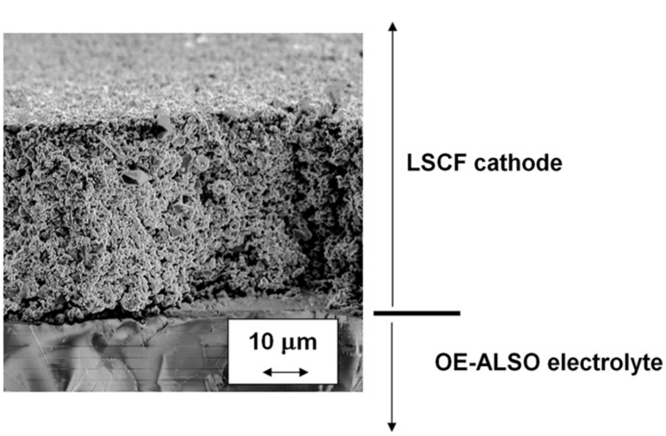

Fig. 3. Cross-sectional SEM image for LSCF/OE-ALSO interface.

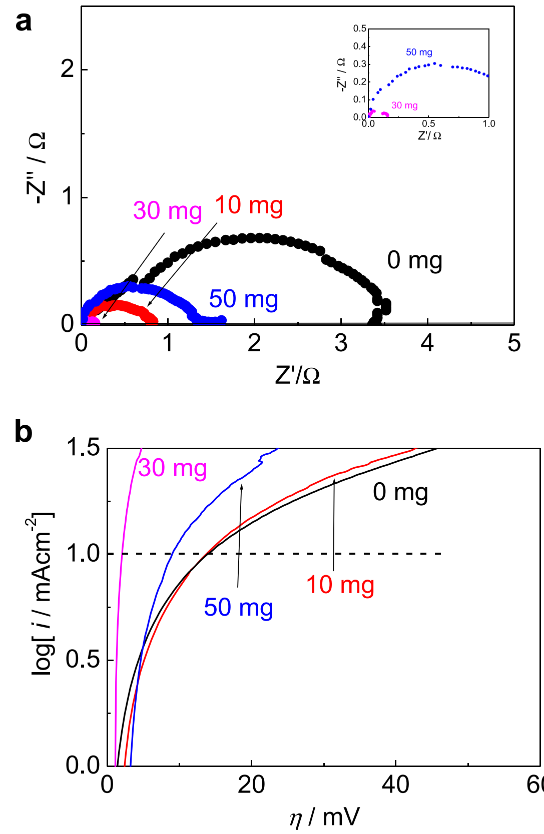

Fig. 4. (a) AC impedance plot (R_{ohml}-free) and (b) DC polarization curve (*IR*-free) for Ag-modified $(La_{0.6}Sr_{0.4})(Co_{0.2}Fe_{0.8})O_{3-\delta}$ electrode/$La_{10}(Si_{5.8}Al_{0.2})O_{26.9}$ (OE-ALSO) electrolyte half cell at 1073 K using a 3-electrode configuration.

3.2. Introduction of Ag nano-particles

There have been many reports for improving the electrocatalytic properties with the introduction of fine noble metals onto the porous electrodes (both cathode and anode) in SOFCs [13,18–20]. In the present study, silver nano-particles were applied on LSCF ($y = 0.8$) particles using the infiltration method, and its effect on the electrochemical behavior of the oxygen-excess-type electrolyte was investigated. The AC impedance and DC polarization results at 1073 K in air for the half cell employing Ag-modified LSCF ($y = 0.8$) electrode are shown in Fig. 4, and obtained data are summarized in Table 2. Similarly, the ohmic resistance, R_{ohm}, and *IR*-loss have been subtracted from the original responses. In each measurement, the LSCF material modified with $M = 30$ mg of the aqueous solution (corresponding to 11 mg of silver) showed the best property, *i.e.* that had the smallest R_{pol} and η. The R_{pol} value for LSCF without silver addition (3.5 Ω) largely decreased with introduction of Ag nano-particles. It could be minimized to 0.2 Ω (0.08 Ω cm^2) in the

Table 2
Evaluated R_{ohm}, R_{pol}, and η from AC impedance and DC polarization methods as a function of amount of $AgNO_3$ aqueous solution (M) in LSCF ($y = 0.8$) for the LSCF/OE-ALSO half cell at 1073 K.

M/mg	R_{ohm}/Ω	R_{pol}/Ω (Ω cm^2)	η/mV at 10 mA cm^{-2}
0	6.5	3.5 (1.3)	14.5
10	3.7	1.3 (0.49)	13.7
30	3.0	0.2 (0.08)	2.1
50	3.1	0.8 (0.3)	4.8

case of $M = 30$ mg even at $y = 0.8$. The current density-cathodic overpotential dependency (Fig. 4b) revealed that the η in air was 2.1 mV at 10 mA cm^{-2} for LSCF with $M = 30$ mg, which was less than two third of that for $y = 0.2$ (Table 1). The η under a current of 0.1 A cm^{-2} at 1073 K was only18 mV for the same system. On the other hand, both R_{pol} and η increased again in the case of $M>30$ mg. The reason might be the densification of silver particles on the top part of the LSCF electrode, preventing transport of oxygen molecules. Wang and Barnett [21] reported the interfacial resistance of $La_{0.7}Sr_{0.3}CoO_3/(Y_2O_3)_{0.25}(Bi_2O_3)_{0.75}$ at 1023 K decreased from 0.7 Ω cm^2 to 0.5 Ω cm^2 by addition of 30% volume fraction of sputtered Ag. Sakito et al. [13] reported the interfacial resistance of $(La_{0.6}Sr_{0.4})(Co_{0.2}Fe_{0.8})O_{3-\delta}/Ce_{0.9}Gd_{0.1}O_{1.9-\delta}$ decreased from 0.63 Ω cm^2 to 0.46 Ω cm^2 at the lower temperature, 803 K, by the silver infiltration technique. In this study, a larger improvement was observed by introduction of very fine silver particles. On the other hand, R_{pol} for the unmodified LSCF electrode in the present study was seemed to be too high. Recently, Muranaka et al. [22] investigated the electrode properties for Ag-$(La_{0.6}Sr_{0.4})(Co_{0.2}Fe_{0.8})O_{3-\delta}$ cermet electrode on the $(La_{0.9}Sr_{0.1})(Ga_{0.8}Mg_{0.2})O_{3-\delta}$ electrolyte. By extrapolating the graph for temperature dependency of the polarization resistance in their report, it was estimated that the R_{pol} values were 0.06 and 0.045 Ω cm^2 at 1073 K for LSCF and Ag-LSCF (50:50 in weight ratio) cermet, respectively. The much lower R_{pol} value for the unmodified LSCF cathode obtained in their study may be due to a suitable current collector/LSCF interface with smaller contact resistance.

As mentioned above, the estimated amount of silver was 11 mg in the case of $M = 30$ mg, which was larger than that for LSCF layer (ca. 7 mg). Although an actual weight of Ag was smaller than the estimated one due to vaporization during the drying process of the silver nitrate solution, the ratio in weight of silver to LSCF is considered to be still high. In the literature [13], the amount of silver in LSCF giving excellent properties was reported to be about 18 wt %. This probably indicates lack of uniformity of silver particles in this study, and even in the case of the modification with 30 mg of solution, the top layer of the LSCF electrode may be largely coated with silver layer. However, this might contribute to a decrease in the contact resistance between the current collector and LSCF. It should be noted that the R_{ohm} also decreased with the solution addition until $M = 30$ mg according to the AC impedance plot as shown in Table 2. This indicates that the introduction of silver resulted in an improvement of the electronic conduction as well as the electrocatalytic activity for the oxygen reduction reaction for $M \leq 30$ mg.

Fig. 5a shows a cross-sectional SEM image (×50,000) of LSCF particles ($M = 30$ mg), applied on the OE-ALSO electrolyte. The enlarged image of the rectangular-shaped region in Fig. 5a is shown in Fig. 5b. Particles of about 60 nm in diameter were observed, without aggregating each other on the LSCF particle. The Auger electron spectra shown in Fig. 5c indicated that the nano-particles observed in Fig. 5b were silver. However, distribution of silver was inhomogeneous from Fig. 5. Since we could not increase the silver amount further to prevent the blocking effect for the gas diffusion, another approaches should be studied in the future. Sakito et al.

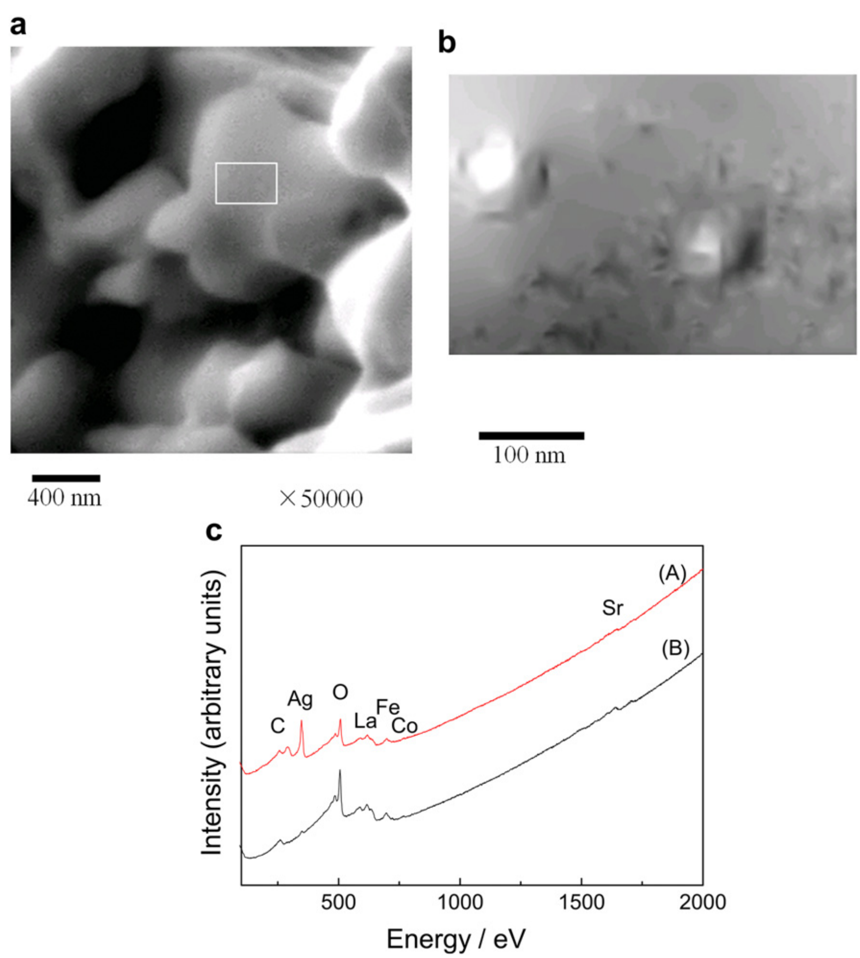

Fig. 5. SEM images and AES spectra for Ag-modified LSCF electrode particles: (a) image of Ag-modified LSCF particles (×50,000 magnification), (b) enlarged image of the rectangular in Fig. 5a, and (c) AES spectra of the LSCF particles: (A) with and (B) without deposition of nano-particles.

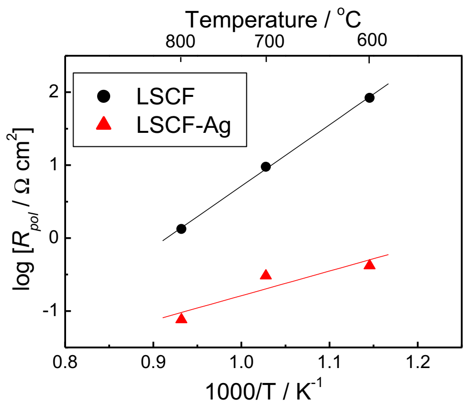

Fig. 6. Temperature dependency of R_{pol} for LSCF and Ag-modified LSCF/ALSO half cells.

[13] reported an improvement of the fuel cell performance for the anode-supported SOFC employing ZrO_2 or CeO_2-based electrolyte by using the Ag (ca. 18 wt.%)-modified LSCF with the same composition as the present study. They reported that the highest power density of the unit cell was observed by using the conditions to form well-distributed Ag fine particles on LSCF by the polymerized complex technique. Although it is necessary to improve homogeneity in the future, it was concluded that the modification technique in the present study is very simple and quite good for fabricating fine silver particles and the contacting layer at the same time, which is also suitable for the oxygen reduction reaction for the oxygen excess-type solid electrolyte.

Fig. 6 shows temperature dependency of R_{pol} ranged between 873 and 1073 K for LSCF with or without silver modification (M = 30 mg). The estimated activation energy for the cathode polarization was 1.68 eV without the modification. This value was almost in agreement with the value found in the literature [22], in which the activation energy of R_{pol} was reported as 1.53 eV for pure LSCF (y = 0.8) on the $(La_{0.9}Sr_{0.1})(Ga_{0.8}Mg_{0.2})O_{3-\delta}$ electrolyte at 773–973 K. This fact may show that there is no big difference in the activation process between oxygen vacancy-type and oxygen excess-type electrolytes, that is, it may be limited by the dissociation process of oxygen molecules. With the modification with 30 mg of $AgNO_3$ solution, the activation energy largely decreased to 0.75 eV. This indicated that the promotion of oxygen dissociation process by the Ag-modification was observed for the oxygen excess-type as well as the oxygen vacancy-type solid electrolyte. Activation energy for the ionic conduction through the OE-ALSO electrolyte is ca. 0.64 eV [10], suggesting that the polarization resistance for the Ag-modified LSCF electrode does not limit the fuel cell performance even for the lower operating temperatures. The Ag-modified LSCF is proved to be a good candidate for the high performance cathode material also for the LSO-based intermediate-temperature SOFCs.

4. Conclusions

Electrochemical oxygen reduction behavior for $(La_{0.6}Sr_{0.4})(Co_{1-y}Fe_y)O_{3-\delta}$, electrode applied on the oxygen excess-type oxide ion conducting solid electrolyte, $La_{10}(Si_{5.8}Al_{0.2})O_{26.9}$ was investigated. The minimum polarization resistance was obtained for y = 0.2. On the other hand, the introduction of silver nano-particles onto the LSCF particles by dropping silver containing solution was quite effective. With the Ag-modification, the R_{pol} could be minimized to 0.08 Ω cm^2 at 1073 K and 0.42 Ω cm^2 at 873 K for y = 0.8. Smaller activation energy for oxygen reduction was obtained in the case of Ag-modified LSCF on the oxygen excess-type solid electrolyte. The cathodic overpotential at 1073 K evaluated from DC polarization was 18 mV at 0.1 A cm^{-2} in that case. The modification technique in the present study is very simple and quite good for fabricating fine silver particles and the contacting layer at the same time, which is suitable for the oxygen reduction reaction also for the oxygen excess-type solid electrolyte, especially at the intermediate temperatures.

Acknowledgment

This study was partially supported by Advanced Low Carbon Technology Research and Development Program (ALCA), from Japan Science and Technology Agency (JST), Japan.

References

[1] S. Nakayama, H. Aono, Y. Sadaoka, Chem. Lett. 24 (1995) 431.
[2] S. Nakayama, T. Kageyama, H. Aono, Y. Sadaoka, J. Mater. Chem. 5 (1995) 1801.
[3] S. Nakayama, M. Sakamoto, J. Eur. Ceram. Soc. 18 (1998) 1413.
[4] M. Higuchi, Y. Masubuchi, S. Nakayama, S. Kikkawa, K. Kodaira, Solid State Ionics 174 (2004) 73.
[5] K. Momma, F. Izumi, J. Appl. Crystallogr. 41 (2008) 653.
[6] H. Arikawa, H. Nishiguchi, T. Ishihara, Y. Takita, Solid State Ionics 31 (2000) 136–137.
[7] H. Yoshioka, Chem. Lett. 33 (2004) 392.
[8] H. Yoshioka, J. Am. Ceram. Soc. 90 (2007) 3099.
[9] A. Mineshige, T. Nakao, M. Kobune, T. Yazawa, H. Yoshioka, Solid State Ionics 179 (2008) 1009.
[10] A. Mineshige, T. Nakao, Y. Ohnishi, R. Sakamoto, Y. Daiko, M. Kobune, T. Yazawa, H. Yoshioka, T. Fukutsuka, Y. Uchimoto, J. Electrochem. Soc. 157 (2010) B1465.
[11] A. Mineshige, Y. Ohnishi, R. Sakamoto, Y. Daiko, M. Kobune, T. Yazawa, H. Yoshioka, T. Nakao, T. Fukutsuka, Y. Uchimoto, Solid State Ionics 192 (2011) 195.
[12] T. Nakao, A. Mineshige, M. Kobune, T. Yazawa, H. Yoshioka, Solid State Ionics 179 (2008) 1567.
[13] Y. Sakito, A. Hirano, N. Imanishi, Y. Takeda, O. Yamamoto, Y. Liu, J. Power Sources 182 (2008) 475.
[14] V.V. Kharton, A.L. Shaula, M.V. Patrakeev, J.C. Waerenborgh, D.P. Rojas, N.P. Vyshatko, E.V. Tsipis, A.A. Yaremchenko, F.M.B. Marques, J. Electrochem. Soc. 151 (8) (2004) A1236.
[15] L.-W. Tai, M.M. Nasrallah, H.U. Anderson, D.M. Sparlin, S.R. Sehlin, Solid State Ionics 76 (1995) 259.
[16] A. Mineshige, M. Inaba, T. Yao, Z. Ogumi, K. Kikuchi, M. Kawase, J. Solid State Chem. 121 (1996) 423.
[17] A. Mineshige, J. Izutsu, M. Nakamura, K. Nigaki, M. Kobune, S. Fujii, M. Inaba, Z. Ogumi, T. Yao, Electrochemistry 68 (2000) 515.
[18] M. Watanabe, H. Uchida, M. Shibata, N. Mochizuki, K. Amikura, J. Electrochem. Soc. 141 (1994) 342.
[19] H. Uchida, N. Mochizuki, M. Watanabe, J. Electrochem. Soc. 143 (1996) 1700.
[20] Y. Liu, M. Mori, Y. Funahashi, Y. Fujishiro, A. Hirano, Electrochem. Commun. 9 (2007) 1918.
[21] L.S. Wang, S.A. Barnett, Solid State Ionics 76 (1995) 103.
[22] M. Muranaka, T. Terai, K. Sasaki, A. Suzuki, J. Electrochem. Soc. 156 (2009) B743.